

## Topological burning glass effect


Simon Körber<sup>1,\*</sup>, Lorenzo Privitera,<sup>1,2</sup> Jan Carl Budich,<sup>3,4</sup> and Björn Trauzettel<sup>1,4</sup>

<sup>1</sup>*Institute of Theoretical Physics and Astrophysics, University of Würzburg, Am Hubland, 97074 Würzburg, Germany*

<sup>2</sup>*Corporate Research, ABB Switzerland Limited, Segelhofstrasse 1K, Baden-Dättwil 5405, Switzerland*

<sup>3</sup>*Institute of Theoretical Physics, Technische Universität Dresden, 01062 Dresden, Germany*

<sup>4</sup>*Würzburg-Dresden Cluster of Excellence ct.qmat, Germany*

 (Received 31 March 2022; revised 5 September 2022; accepted 30 September 2022; published 20 October 2022)

We reveal a topological burning glass effect, where the local response of a system exhibits a topological quantization that is enhanced by an integer due to its environmental coupling. As a paradigmatic platform for this intriguing phenomenon, we study a central spin that is quasiperiodically driven by two incommensurate frequencies, and statically coupled to  $N - 1$  surrounding spins. In the strong-coupling regime, the adiabatic dynamics of the total system is readily understood to imprint on the central spin an  $N$ -fold enhanced topological frequency conversion between the two driving frequencies. We argue that the topological burning glass effect is induced by the nonunitary dynamics of the central spin, which locally involves the collective motion of the surrounding spins. Our results are derived in the framework of adiabatic perturbation theory and fully corroborated by exact numerical simulations.

DOI: [10.1103/PhysRevB.106.L140304](https://doi.org/10.1103/PhysRevB.106.L140304)

*Introduction.* Geometry and topology have been identified to be at the heart of some of the most fascinating phenomena in physics [1–4]. A paradigmatic example is provided by the quantum Hall effect [5,6], where an impressively precise quantization of the transverse conductance in two-dimensional (2D) systems has been explained with theory in terms of a topological invariant characterizing the underlying electronic state [7–10].

Generally speaking, linear response properties such as the aforementioned Hall conductance are governed by the celebrated Kubo formula [11,12]. When interpreted as a dynamical expression, linear response ostensibly refers to the first perturbative correction of the state due to an external field. However, as an equilibrium property, it can eventually be understood in terms of the unperturbed state alone. Returning to the integer quantum Hall effect, the topologically quantized response is thus characterized by the first Chern number [8,13–17], an invariant defined in terms of the adiabatic Berry curvature [18] of the occupied Bloch bands exclusively referring to the ground state of the system.

In this Letter, we reveal how this correspondence between adiabatically defined topological invariants and quantized response properties is fundamentally modified in open quantum systems. To this end, we extend the Floquet counterpart of an integer quantum Hall system [19], i.e., a spin driven with two incommensurate frequencies, by statically coupling it to a set of surrounding spins in the framework of a central spin model (CSM) [20–22] (see Fig. 1). In this system, the topologically quantized response is given by the energy transfer between the two driving modes, which represents a local observable of the driven central spin. Yet, the adiabatically defined Chern

number of the central spin fails to predict the linear response signal, which can instead only be topologically understood from the adiabatic state of the total system. In this sense, the topological properties of the environmental spins are focused to the local response of the central spin, motivating the terminology of a topological burning glass. We argue that the topological burning glass effect generically occurs in any static extension of the CSM under the following three conditions: (i) The initial state of the interacting spin system is energetically separated from the other bands, (ii) the dynamics is well described within first-order adiabatic perturbation theory [23,24], and (iii) the time-quasiperiodic fields only act on the central spin. In our concrete topological burning glass scenario, the quantized energy transfer is found to be  $N$ -fold enhanced by the collective motion of  $N$  spins, while the adiabatic Chern number of the driven spin remains equal to one. Our analytical results are corroborated by numerically exact simulations, which also allow us to systematically study the breakdown of the adiabatic dynamics in our model. This nonadiabatic breakdown occurs when the driving frequencies approach the size of the energy gap above the many-body ground state that generically scales as  $1/N$  in our model.

*Model and adiabatic perturbation theory.* We consider the dynamics of a central spin that is subjected to a time-quasiperiodic magnetic field  $\mathbf{B}(\vec{\varphi}_t)$ , and interacts in a static fashion with its environment. A minimal framework for this scenario is provided by the following driven CSM (see Fig. 1 for an illustration),

$$\hat{H}(\vec{\varphi}_t) = g^* \mu_B \mathbf{B}(\vec{\varphi}_t) \cdot \hat{\mathbf{S}}_0 - A \hat{\mathbf{S}}_0 \cdot \hat{\mathbf{J}}, \quad (1)$$

where  $\hat{\mathbf{S}}_0 = \frac{1}{2} \hat{\sigma}_0$  represents the central spin-1/2 and  $\hat{\mathbf{J}} = \sum_{k=1}^{N-1} \hat{\mathbf{S}}_k = \sum_{k=1}^{N-1} \frac{\hat{\sigma}_k}{2}$  the surrounding spins. The environment is composed of a number of  $N - 1$  spin-1/2, and is assumed

\*skoerber@physik.uni-wuerzburg.de

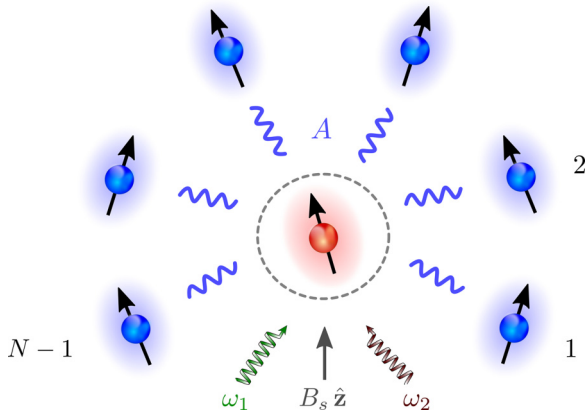


FIG. 1. Quasiperiodically driven central spin model (CSM) as a topological burning glass. A central spin (red sphere) couples in star geometry to  $N - 1$  surrounding spins (blue spheres). The isotropic interaction is parametrized by the homogeneous coupling constant  $A$ . The central spin is subjected to a static magnetic field with amplitude  $B_s$  and two circularly polarized drives with incommensurate frequencies  $\omega_1$  and  $\omega_2$ , so as to induce a topological frequency conversion.

to interact homogeneously with the central spin with coupling strength  $A$ . We have set  $\hbar = 1$  and introduced the vector of Pauli matrices  $\hat{\sigma}_i = (\hat{\sigma}_i^x, \hat{\sigma}_i^y, \hat{\sigma}_i^z)$  acting on the individual subspaces of the constituents. The Zeeman term generated by the magnetic field  $\mathbf{B}(\vec{\varphi}_t)$  is proportional to Bohr's magneton  $\mu_B$  and the effective  $g^*$  factor of the central spin. This model effectively applies for instance to driven electron spins trapped in lateral quantum dots in SiGe or nitrogen-vacancy (NV) centers in diamond [25]. In these systems, the (central) electron spin couples in a starlike fashion to the surrounding nuclear spins of the host material, with a hyperfine interaction that is typically three orders of magnitude larger than the dipole-dipole coupling between the nuclear spins themselves [26–28].

The time dependence of the external field  $\mathbf{B}(\vec{\varphi}_t) = B_c \mathbf{d}(\vec{\varphi}_t)$  is chosen as [10,19,29]

$$\mathbf{d}(\vec{\varphi}_t) = \begin{pmatrix} \sin(\varphi_{1t}) \\ \sin(\varphi_{2t}) \\ M - \cos(\varphi_{1t}) - \cos(\varphi_{2t}) \end{pmatrix}.$$

It consists of a static magnetic field with amplitude  $B_s = B_c M$  in the  $z$  direction, and two circularly polarized drives, with amplitudes  $B_c$  and time-dependent phases  $\vec{\varphi}_t = (\varphi_{1t}, \varphi_{2t}) = \vec{\omega} t + \vec{\phi}$ . The offset phases and incommensurate frequencies are parametrized by  $\vec{\phi} = (\phi_1, \phi_2)$  and  $\vec{\omega} = (\omega_1, \omega_2)$ .

In order to cope with the influence of the surrounding spins, we take advantage of the homogeneity of the interaction based on the starlike symmetry of Eq. (1), that entails  $[\hat{H}(\vec{\varphi}_t), \hat{\mathbf{J}}^2] = 0$ . The Hamiltonian  $\hat{H}(\vec{\varphi}_t)$  may thus be transformed into a block diagonal form, with each block characterized by a constant of motion,

$$j = \begin{cases} \frac{N-1}{2}, \frac{N-1}{2} - 1, \dots, \frac{1}{2}, & N \text{ even,} \\ \frac{N-1}{2}, \frac{N-1}{2} - 1, \dots, 0, & N \text{ odd,} \end{cases}$$

corresponding to the total spin  $\hat{\mathbf{J}}^2$  of the surrounding spins with  $N \geq 2$ . As we want to focus on the dynamics originating

from the ground state, we restrict ourselves to the block  $j = \frac{N-1}{2}$  [30]. The associated block matrix size is  $2N \times 2N$ , and the instantaneous spectrum is obtained by solving

$$\hat{H}(\vec{\varphi}_t) |\Phi_\alpha(\vec{\varphi}_t)\rangle = E_\alpha(\vec{\varphi}_t) |\Phi_\alpha(\vec{\varphi}_t)\rangle. \quad (2)$$

The energies  $E_\alpha(\vec{\varphi}_t)$  are ordered from low to high values by ascending indices  $\alpha = 0, 1, \dots, 2N - 1$ , where  $\alpha = 0$  denotes the ground state. For an incommensurate pair of frequencies  $\frac{\omega_1}{\omega_2} \notin \mathbb{Q}$ , the phases  $\varphi_{1t}$  and  $\varphi_{2t}$  sample entirely the surface of a two-dimensional torus, analogously to a synthetic 2D Brillouin zone (BZ). The energy levels  $E_\alpha(\vec{\varphi}_t)$  then resemble a band structure in parameter space, with the phases  $\vec{\varphi}_t$  taking the role of Bloch quasimomenta. Assuming that the interacting spin system is gapped [30] and initially prepared in an instantaneous eigenstate  $|\Phi_\beta(\vec{\varphi}_0)\rangle$  of Eq. (2), the dynamics can be expanded to first order in  $\vec{\omega}$  using adiabatic perturbation theory [23,24]:

$$|\Psi_\beta(t)\rangle = e^{i\gamma_\beta(t)} \left[ |\Phi_\beta(\vec{\varphi}_t)\rangle + i \sum_{\alpha \neq \beta} \frac{\mathcal{M}_{\alpha\beta}(\vec{\varphi}_t)}{\Delta_{\alpha\beta}(\vec{\varphi}_t)} |\Phi_\alpha(\vec{\varphi}_t)\rangle \right]. \quad (3)$$

At zeroth order, the quantum state  $|\Psi_\beta(t)\rangle$  is restricted to the synthetic energy band  $E_\beta(\vec{\varphi}_t)$ . First-order corrections, however, yield virtual transitions to the excited states of the instantaneous spectrum, weighted by the terms  $\mathcal{M}_{\alpha\beta}(\vec{\varphi}_t) = \vec{\omega} \langle \Phi_\alpha(\vec{\varphi}_t) | \nabla_{\vec{\varphi}} \Phi_\beta(\vec{\varphi}_t) \rangle$  and the energy gaps  $\Delta_{\alpha\beta}(\vec{\varphi}_t) = E_\alpha(\vec{\varphi}_t) - E_\beta(\vec{\varphi}_t)$ . We have also introduced the overall phase factor  $\gamma_\beta(t) = -\int_{t_0}^t dt' [E_\beta(\vec{\varphi}_{t'}) - i \mathcal{M}_{\beta\beta}(\vec{\varphi}_{t'})]$ .

*Topological frequency conversion.* A feature of quasiperiodically driven systems is energy pumping, a process in which photons of different frequencies are exchanged between the external drives [19,31–44]. The total energy transfer rate is determined by the equations of motion:  $\frac{d}{dt} \langle \hat{H} \rangle = \langle \partial_t \hat{H} \rangle = \vec{\omega} \langle \hat{\mathbf{I}} \rangle$ , with  $\hat{\mathbf{I}} = (\hat{\mathbf{I}}_1, \hat{\mathbf{I}}_2) = \nabla_{\vec{\varphi}} \hat{H}$ . Each term  $\omega_k \langle \hat{\mathbf{I}}_k \rangle$  can be interpreted as the pumping rate provided by the individual drive, where  $\hat{\mathbf{I}}_k = \partial_{\varphi_k} \hat{H}$  resembles a current operator in the  $k$  direction of the parameter space. Using the perturbed quantum state  $|\Psi_\beta(t)\rangle$  from Eq. (3), the expectation value  $\langle \hat{\mathbf{I}}_k \rangle$  can be expanded to first order in  $\vec{\omega}$  [24,45]:

$$\langle \hat{\mathbf{I}}_k \rangle_\beta = \langle \Psi_\beta | \hat{\mathbf{I}}_k | \Psi_\beta \rangle = \frac{\partial E_\beta}{\partial \varphi_k} + \sum_{l=1}^2 \omega_l \Omega_{kl}^{(\beta)}. \quad (4)$$

This result emphasizes that virtual couplings between bands are essential for the generation of geometrical and topological effects, as the adiabatic limit only produces Bloch oscillations  $\partial_{\varphi_k} E_\beta$  [46]. In fact, the virtual interband excitations of Eq. (3) can be readily shown to be identical to the Berry curvature  $\Omega_{kl}^{(\beta)}(\vec{\varphi}_t) = 2 \text{Im}[\langle \partial_{\varphi_k} \Phi_\beta(\vec{\varphi}_t) | \partial_{\varphi_l} \Phi_\beta(\vec{\varphi}_t) \rangle]$  of the synthetic energy band  $E_\beta(\vec{\varphi}_t)$  to which the adiabatic dynamics is confined. This phenomenon demonstrates that, in an isolated quantum system, the Berry curvature  $\Omega_{kl}^{(\beta)}$  arises as the adiabatic first-order response of a physical observable ( $\hat{\mathbf{I}}_k = \partial_{\varphi_k} \hat{H}$ ) to the rate of change of the external parameter (e.g.,  $\dot{\vec{\varphi}}_t = \vec{\omega}$ ) [24,45].

As the two frequencies  $\frac{\omega_1}{\omega_2} \notin \mathbb{Q}$  are incommensurate, the entire synthetic 2D BZ is sampled during the time evolution of the quantum state  $|\Psi_\beta(t)\rangle$ . Averaging the pumping rates of Eq. (4) over a long period of time, this translates into an integration over the closed manifold of the

two-dimensional torus. The Bloch oscillations do not contribute to this integration, while the integrated Berry curvature produces a topological frequency conversion between the dynamical drives that is proportional to the first Chern number  $C^{(\beta)} = \frac{1}{2\pi} \iint_0^{2\pi} d^2\vec{\varphi} \Omega_{12}^{(\beta)}(\vec{\varphi})$ . The time-averaged pumping rate yields [19]

$$P_{\beta}^{12} = -P_{\beta}^{21} = \frac{C^{(\beta)}}{2\pi} \omega_1 \omega_2. \quad (5)$$

The topologically quantized response of the total quantum system of Eq. (1) is thus characterized by its adiabatically defined topological invariant  $C^{(\beta)}$ . We contrast this behavior with its counterpart in an open quantum system in the next section.

*Burning glass effect.* We take an open quantum system perspective, in which a physical observable of interest operates locally on the (small) quantum system that is coupled to a (larger) environment. Specifically, in Eq. (1), only the central spin is exposed to the quasiperiodic field  $\mathbf{B}(\vec{\varphi}_t)$ , resulting in a current operator  $\hat{I}_k = \lambda \frac{\partial \mathbf{d}(\vec{\varphi}_t)}{\partial \varphi_k} \cdot \hat{\mathbf{S}}_0$  that acts exclusively on the central spin-1/2. Accordingly, the expectation value

$$\langle \hat{I}_k \rangle_{\beta} = \text{Tr}[\hat{\rho}_{\beta}^{\text{dy}} \hat{I}_k] = \text{Tr}_0[\hat{\rho}_{0,\beta}^{\text{dy}} \hat{I}_k] \quad (6)$$

can be fully determined by the nonunitary dynamics of the central spin, expressed by the reduced density matrix  $\hat{\rho}_{0,\beta}^{\text{dy}}(t) = \text{Tr}_{\mathbf{j}}[\hat{\rho}_{\beta}^{\text{dy}}(t)]$ . Here, we have introduced the total density matrix  $\hat{\rho}_{\beta}^{\text{dy}}(t) = |\Psi_{\beta}(t)\rangle\langle\Psi_{\beta}(t)|$ , where  $|\Psi_{\beta}(t)\rangle$  represents the perturbed quantum state of Eq. (3) [47]. The reduced density matrix is calculated by tracing out the environment  $\hat{\mathbf{J}}$  (denoted as  $\text{Tr}_{\mathbf{j}}$ ), while  $\text{Tr}$  ( $\text{Tr}_0$ ) denotes the trace operating on the total system (the central spin-1/2). We have further introduced the energy scale

$$\lambda = g^* \mu_B B_c,$$

assuming  $\lambda > 0$  for simplicity.

Equation (6) illustrates that the frequency conversion is entirely carried by the central spin. The topological quantization of the local response, however, is determined by the geometrical and topological properties of the total system, namely the Berry curvature  $\Omega_{kl}^{(\beta)}$  and the Chern number  $C^{(\beta)}$  of the synthetic energy band  $E_{\beta}(\vec{\varphi}_t)$  to which the adiabatic dynamics is confined. Thus, the nonunitary dynamics of the central spin effectively inherits the topological nature of the total system. Employing the perturbed quantum state  $|\Psi_{\beta}(t)\rangle$  of Eq. (3), this phenomenon can be further analyzed by a first-order expansion in  $\vec{\omega}$  of the reduced density matrix

$$\hat{\rho}_{0,\beta}^{\text{dy}}(t) = \hat{\rho}_{0,\beta}^{\text{ad}}(t) + \sum_{\alpha \neq \beta} \frac{\hat{T}_{\alpha\beta}(\vec{\varphi}_t)}{\Delta_{\alpha\beta}(\vec{\varphi}_t)}. \quad (7)$$

Here, we introduce the adiabatic limit of the reduced density matrix  $\hat{\rho}_{0,\beta}^{\text{ad}} = \text{Tr}_{\mathbf{j}}[|\Phi_{\beta}\rangle\langle\Phi_{\beta}|]$ , which corresponds to the zeroth order of Eq. (3), and results in Bloch oscillations  $\partial_{\varphi_k} E_{\beta}$  of Eq. (4). The local response, however, arises from the operators  $\hat{T}_{\alpha\beta} = i \mathcal{M}_{\alpha\beta} \text{Tr}_{\mathbf{j}}[|\Phi_{\alpha}\rangle\langle\Phi_{\beta}|] + \text{H.c.}$  accounting for the virtual transitions to the excited states in the instantaneous spectrum of the total system. In fact, the correlations of the total system are manifested in the matrix elements of  $\hat{T}_{\alpha\beta}$ , thus imposing a

topological quantization that is not captured by basic geometrical or topological aspects of the reduced adiabatic density matrix  $\hat{\rho}_{0,\beta}^{\text{ad}}$ . In this sense, the adiabatic topological properties of the total system are focused to the local response of the central spin, which motivates the terminology of a topological burning glass. This mechanism is quite generic, since Eqs. (2)–(7) reflect fundamental concepts that do not depend on the details of the model. Instead, it is only assumed that the adiabatic dynamics starts from a gapped synthetic energy band of the total system, and that the physical observable of interest operates locally on the (small) quantum system. The robustness of our results to more generic couplings is further corroborated in the Supplemental Material (SM) [30].

To further analyze the topological burning glass effect, we contrast the dynamics of a decoupled central spin with the collective dynamics in the strong-coupling regime. We start with the noninteracting case, where Eq. (1) transforms into a single-spin Hamiltonian resembling the momentum-space representation of a Chern insulator [10,29] with mass parameter  $M$ . Thus, each of the two single-spin energy bands can be characterized by a Chern number [8,13–17]:  $\nu_{\text{gr}} = -\nu_{\text{ex}} = \pm 1$  (nontrivial) for  $|M| < 2$ ,  $M \neq 0$  or  $\nu_{\text{gr}} = \nu_{\text{ex}} = 0$  (trivial) for  $|M| > 2$ , where  $\nu_{\text{gr}}$  ( $\nu_{\text{ex}}$ ) corresponds to the single-spin ground (excited) energy band. Starting from the single-spin ground state, the adiabatic dynamics produces a topological frequency conversion that is proportional to  $\nu_{\text{gr}} = -\frac{1}{4\pi} \iint_0^{2\pi} d^2\vec{\varphi} \tilde{\mathbf{d}}(\vec{\varphi}) [\partial_{\varphi_1} \tilde{\mathbf{d}}(\vec{\varphi}) \times \partial_{\varphi_2} \tilde{\mathbf{d}}(\vec{\varphi})]$  with  $\tilde{\mathbf{d}}(\vec{\varphi}) = \frac{\mathbf{d}(\vec{\varphi})}{|\mathbf{d}(\vec{\varphi})|}$ . In the interacting case, the interaction effectively extends the magnetic coupling to the surrounding spins, forcing them to rotate along the direction of the external field  $\mathbf{B}(\vec{\varphi}_t)$  as well. In the strong-coupling regime and for ferromagnetic coupling strength  $A > 0$  [30], this collective behavior imposes a topological frequency conversion that is proportional [cf. Eq. (5)] to the total Chern number

$$C^{(0)} = N \nu_{\text{gr}} \quad (8)$$

of the ferromagnetic ground state. This behavior affords a simple interpretation: In the adiabatic limit, the surrounding spins point in the same direction as the central spin at every point in time, such that each spin contributes to the many-body wave function by the same single-spin Chern number  $\nu_{\text{gr}}$ . Importantly, the adiabatic ground state is a product state at all times, such that the reduced adiabatic density matrix  $\hat{\rho}_{0,0}^{\text{ad}} = \frac{1}{2} [1 - \tilde{\mathbf{d}}(\vec{\varphi}) \cdot \hat{\sigma}]$  yields a Chern number  $\nu_{\text{gr}}$  that is given by that of a single spin-1/2. The latter thus fails to capture the topological quantization and enhancement of the local response, revealing a burning glass effect in which the aforementioned collective motion of all spins is locally imprinted in the nonunitary dynamics of the central spin. In fact, as we describe in the SM [30], the operators  $\hat{T}_{\alpha\beta}$  of Eq. (7) induce fluctuations around the adiabatic spin polarization of the central spin-1/2, including the topological information of the total system, and affecting the indirect measurement of the topological frequency conversion [48–50].

*Numerical simulations.* We corroborate the formation of a topological burning glass by numerically solving the Schrödinger equation associated with  $\hat{H}$  up to times  $\lambda T = 5 \times 10^5$  [51]. If the initial state at  $t_0 = 0$  corresponds to the ferromagnetic ground state, the time-averaged pumping

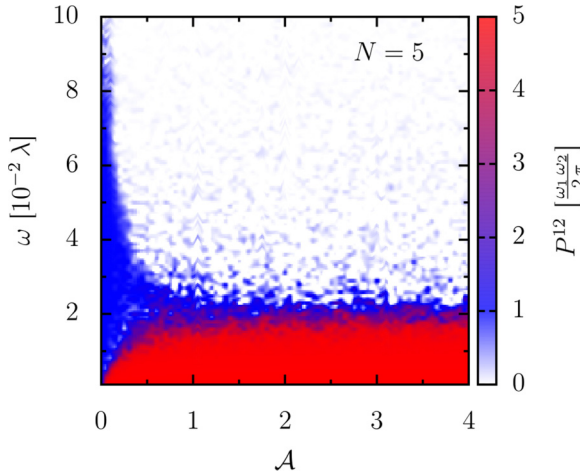


FIG. 2. Nonequilibrium phase diagram as a function of interaction strength  $\mathcal{A} > 0$  and frequencies  $\omega_1 = \omega$ ,  $\omega_2 = \gamma \omega$  for  $N = 5$ . The mass parameter  $M = 1.2$  is chosen in the nontrivial topological regime ( $\nu_{\text{gr}} = 1$ ). Provided the adiabatic dynamics is confined to the ferromagnetic ground state, the time-averaged pumping rate  $P^{12}$  is proportional to the Chern number  $C^{(0)} = N \nu_{\text{gr}}$  (red regime). Nonadiabatic excitations can result in transitions to intermediate/featureless quantum phases with pumping rates  $\bar{P}^{12} = \frac{\nu_{\text{gr}}}{2\pi} \omega_1 \omega_2$  (blue regime)/ $P^{12} = 0$  (white regime).

rate  $P^{12}$  can be extrapolated by the gradient [52] of the energy transfer  $W_1(t) = \omega_1 \int_0^t dt' \langle \hat{I}_1(t') \rangle$ . In Fig. 2, the pumping rate  $P^{12}$  is shown as a function of ferromagnetic interaction strength  $\mathcal{A} > 0$  [30] and frequency  $\omega$  for a total number of spins  $N = 5$ , where we have introduced the renormalized interaction strength  $\mathcal{A} = A/\lambda$ . The mass parameter  $M = 1.2$  is selected such that the system is in the nontrivial topological regime, yielding an adiabatic Chern number  $\nu_{\text{gr}} = 1$  of the driven spin. We have chosen the frequencies  $\omega_1 = \omega$  and  $\omega_2 = \gamma \omega$ , where  $\gamma = \frac{1}{2}(1 + \sqrt{5})$  is the golden ratio. The offset phases are  $\phi_1 = \pi/10$ ,  $\phi_2 = 0$ .

A finite interaction strength drives the system into the burning glass regime with an  $N$ -fold enhanced topological frequency conversion determined by the Chern number of Eq. (8) (red regime). Away from the zero-frequency limit, there exist parameter ranges at which the strong-coupling regime of Eq. (5) breaks down. The dynamics leads to nonadiabatic excitation processes between the instantaneous eigenstates of the spectrum, yielding a suppression of the dynamical

response. Finally, the system enters an ergodic regime that leads to a featureless state with pumping rate  $P^{12} = 0$  (white regime). Interestingly, in the CSM, there exists an intermediate dynamical quantum phase in which the spectrum is only partially occupied. The topological frequency conversion then even extends to a nonadiabatic situation, with a pumping rate  $\bar{P}^{12} = \frac{\nu_{\text{gr}}}{2\pi} \omega_1 \omega_2$  similar to that of the single spin (blue regime). A detailed description of the nonadiabatic breakdown of the strong-coupling regime is presented in the SM [30], showing that the parameter ranges of the nonequilibrium phase diagram mainly depend on the relations between the driving frequencies and the energy gaps of the band structure. More precisely, the phase boundaries in Fig. 2 are approximately covered by critical frequencies proportional to the energy gaps separating the spectrum into the aforementioned dynamical quantum phases. Note that these energy gaps scale with  $1/N$ , indicating that the topological burning glass effect represents a finite-size effect in our model.

*Conclusion.* We have discovered a topological burning glass effect, in which the local response of a quantum system exhibits a topological quantization that is enhanced by an integer due to its environmental coupling. The quantum system adopts the topological nature of the total system in its nonunitary dynamics, imposing a local response that cannot be captured by its reduced adiabatic density matrix. We expect that this intriguing phenomenon exemplifies a more general principle of topological open quantum systems.

As a prototypical example of a topological burning glass, we have studied energy pumping in a quasiperiodically driven central spin model. In the strong-coupling regime, the central spin experiences a magnification of the topological frequency conversion that is significantly enhanced with the number of surrounding spins. This amplification could be exploited to enable the direct experimental observation of a quantized energy current, providing a complementary approach to the recent suggestions made in the context of Weyl semimetals [53].

*Acknowledgments.* This work was supported by the DFG [SPP1666, SFB1170 “ToCoTronics”, SFB 1143 (project-id 247310070), and DFG Project No. 419241108], the Würzburg-Dresden Cluster of Excellence ct.qmat (EXC2147, Project No. 390858490), and the Elitenetzwerk Bayern Graduate School on “Topological Insulators.” The computational work presented in this Letter was performed on the Würzburg HPC cluster.

- [1] D. J. Thouless, *Topological Quantum Numbers in Nonrelativistic Physics* (World Scientific, Singapore, 1998).
- [2] D. Xiao, M.-C. Chang, and Q. Niu, *Rev. Mod. Phys.* **82**, 1959 (2010).
- [3] X.-G. Wen, *Rev. Mod. Phys.* **89**, 041004 (2017).
- [4] J. Cayssol and J. N. Fuchs, *J. Phys.: Mater.* **4**, 034007 (2021).
- [5] K. v. Klitzing, G. Dorda, and M. Pepper, *Phys. Rev. Lett.* **45**, 494 (1980).
- [6] R. E. Prange and S. M. Girvin, *The Quantum Hall Effect*, 2nd ed. (Springer, New York, 1990).
- [7] R. B. Laughlin, *Phys. Rev. B* **23**, 5632 (1981).

- [8] D. J. Thouless, M. Kohmoto, M. P. Nightingale, and M. den Nijs, *Phys. Rev. Lett.* **49**, 405 (1982).
- [9] B. Simon, *Phys. Rev. Lett.* **51**, 2167 (1983).
- [10] F. D. M. Haldane, *Phys. Rev. Lett.* **61**, 2015 (1988).
- [11] R. Kubo, *J. Phys. Soc. Jpn.* **12**, 570 (1957).
- [12] G. D. Mahan, *Many-Particle Physics*, 3rd ed. (Kluwer, Boston, 2000).
- [13] S. S. Chern, *Ann. Math.* **47**, 85 (1946).
- [14] X.-L. Qi, T. L. Hughes, and S.-C. Zhang, *Phys. Rev. B* **78**, 195424 (2008).
- [15] M. Z. Hasan and C. L. Kane, *Rev. Mod. Phys.* **82**, 3045 (2010).

- [16] X.-L. Qi and S.-C. Zhang, *Rev. Mod. Phys.* **83**, 1057 (2011).
- [17] B. A. Bernevig and T. L. Hughes, *Topological Insulators and Topological Superconductors* (Princeton University Press, Princeton, NJ, 2013).
- [18] M. V. Berry, *Proc. R. Soc. London, Ser. A* **392**, 45 (1984).
- [19] I. Martin, G. Refael, and B. Halperin, *Phys. Rev. X* **7**, 041008 (2017).
- [20] M. Gaudin, *J. Phys. France* **37**, 1087 (1976).
- [21] J. Dukelsky, S. Pittel, and G. Sierra, *Rev. Mod. Phys.* **76**, 643 (2004).
- [22] P. W. Claeys, C. Dimo, S. D. Baerdemacker, and A. Faribault, *J. Phys. A: Math. Theor.* **52**, 08LT01 (2019).
- [23] G. Rigolin, G. Ortiz, and V. H. Ponce, *Phys. Rev. A* **78**, 052508 (2008).
- [24] P. Weinberg, M. Bukov, L. D'Alessio, A. Polkovnikov, S. Vajna, and M. Kolodrubetz, *Phys. Rep.* **688**, 1 (2017).
- [25] In lateral quantum dots or NV centers, the Heisenberg interaction to the surrounding spins is not necessarily isotropic, as assumed for simplicity in Eq. (1). However, as our main statements about the topological burning glass effect reflect fundamental concepts that do not depend on the details of the model, our results generally apply to anisotropic interactions as well.
- [26] R. Hanson, L. P. Kouwenhoven, J. R. Petta, S. Tarucha, and L. M. K. Vandersypen, *Rev. Mod. Phys.* **79**, 1217 (2007).
- [27] M. W. Doherty, N. B. Manson, P. Delaney, F. Jelezko, J. Wrachtrup, and L. C. Hollenberg, *Phys. Rep.* **528**, 1 (2013).
- [28] A. Chatterjee, P. Stevenson, S. De Franceschi, A. Morello, N. P. de Leon, and F. Kuemmeth, *Nat. Rev. Phys.* **3**, 157 (2021).
- [29] X.-L. Qi, Y.-S. Wu, and S.-C. Zhang, *Phys. Rev. B* **74**, 085308 (2006).
- [30] See Supplemental Material at <http://link.aps.org/supplemental/10.1103/PhysRevB.106.L140304> for additional technical details about the central spin model (CSM), including the derivation of the instantaneous spectrum of the interacting spin system (Sec. A), the stability analysis for more generic extensions of the CSM (Sec. B), the illustration of the fluctuations around the adiabatic spin polarization of the central spin-1/2 (Sec. C), the detailed description of the nonadiabatic breakdown of the strong-coupling regime with the associated scaling behavior (Sec. D), and the results for antiferromagnetic coupling strength  $A < 0$  (Sec. E).
- [31] M. H. Kolodrubetz, F. Nathan, S. Gazit, T. Morimoto, and J. E. Moore, *Phys. Rev. Lett.* **120**, 150601 (2018).
- [32] Y. Peng and G. Refael, *Phys. Rev. B* **97**, 134303 (2018).
- [33] P. J. D. Crowley, I. Martin, and A. Chandran, *Phys. Rev. B* **99**, 064306 (2019).
- [34] F. Nathan, I. Martin, and G. Refael, *Phys. Rev. B* **99**, 094311 (2019).
- [35] S. Körber, L. Privitera, J. C. Budich, and B. Trauzettel, *Phys. Rev. Res.* **2**, 022023(R) (2020).
- [36] P. J. D. Crowley, I. Martin, and A. Chandran, *Phys. Rev. Lett.* **125**, 100601 (2020).
- [37] E. Boyers, P. J. D. Crowley, A. Chandran, and A. O. Sushkov, *Phys. Rev. Lett.* **125**, 160505 (2020).
- [38] Q. Chen, H. Liu, M. Yu, S. Zhang, and J. Cai, *Phys. Rev. A* **102**, 052606 (2020).
- [39] F. Nathan, G. Refael, M. S. Rudner, and I. Martin, *Phys. Rev. Res.* **2**, 043411 (2020).
- [40] D. M. Long, P. J. D. Crowley, and A. Chandran, *Phys. Rev. Lett.* **126**, 106805 (2021).
- [41] F. Nathan, R. Ge, S. Gazit, M. Rudner, and M. Kolodrubetz, *Phys. Rev. Lett.* **127**, 166804 (2021).
- [42] C. Psaroudaki and G. Refael, *Ann. Phys.* **435**, 168553 (2021).
- [43] Z. Qi, G. Refael, and Y. Peng, *Phys. Rev. B* **104**, 224301 (2021).
- [44] K. Schwennicke and J. Yuen-Zhou, *J. Phys. Chem. Lett.* **13**, 2434 (2022).
- [45] V. Gritsev and A. Polkovnikov, *Proc. Natl. Acad. Sci. USA* **109**, 6457 (2012).
- [46] F. Bloch, *Z. Phys.* **52**, 555 (1929).
- [47] Note that Eq. (6) also holds for the exact dynamics of the system, involving the higher orders in the perturbative expansion of Eq. (3).
- [48] M. D. Schroer, M. H. Kolodrubetz, W. F. Kindel, M. Sandberg, J. Gao, M. R. Vissers, D. P. Pappas, A. Polkovnikov, and K. W. Lehnert, *Phys. Rev. Lett.* **113**, 050402 (2014).
- [49] P. Roushan, C. Neill, Y. Chen, M. Kolodrubetz, C. Quintana, N. Leung, M. Fang, R. Barends, B. Campbell, Z. Chen, B. Chiaro, A. Dunsworth, E. Jeffrey, J. Kelly, A. Megrant, J. Mutus, P. J. J. O'Malley, D. Sank, A. Vainsencher, J. Wenner *et al.*, *Nature (London)* **515**, 241 (2014).
- [50] D. Malz and A. Smith, *Phys. Rev. Lett.* **126**, 163602 (2021).
- [51] For a time  $\lambda T = 5 \times 10^5$ , the entire synthetic 2D Brillouin zone (BZ) is sufficiently sampled for our choice of parameters.
- [52] We obtain the gradient by computing  $P^{12} = \frac{2}{T} (\bar{W}_1^T - \bar{W}_1^{T/2})$  with the time-averaged energy transfers  $\bar{W}_1^{T/2} = \frac{2}{T} \int_0^{T/2} dW_1(t)$  and  $\bar{W}_1^T = \frac{2}{T} \int_{T/2}^T dt W_1(t)$ .
- [53] F. Nathan, I. Martin, and G. Refael, [arXiv:2201.07804](https://arxiv.org/abs/2201.07804) [Phys. Rev. Res. (to be published)].